COBEM 2023 27TH INTERNATIONAL CONGRESS OF MECHANICAL ENGENEERING

ABCM Brazilian Society of Mechanical Sciences and Engineering
27th ABCM International Congress of Mechanical Engineering
December 04-08, 2023, Florianópolis-SC, Brazil

COB-2023-2003
NUMERICAL MODEL OF THE TETRAHYDROFURAN HYDRATE GROWTH KINETIC

Gino Noel Delgado Dextre
Ernesto Mancilla
Moises Alves Marcelino Neto
Rigoberto Eleazar Melgarejo Morales
Multiphase Flow Research Center – NUEM, Pos Graduate Program in Mechanical Engineering – PPGEM, Federal University of Technology of Parana, Brazil
gdelgadodextre@gamil.com
faermara@hotmail.com
mneto@utfpr.edu.br
rmorales@utfpr.edu.br

Abstract. *This study introduces a numerical model that utilizes an analytical approach to describe the growth of tetrahydrofuran hydrate, incorporating heat transfer, mass transfer, and chemical kinetics. The model establishes relationships among these factors, providing a comprehensive understanding of the growth process and the interplay between heat transfer, mass transfer, and chemical reactions. The model was implemented as User Defined Functions (UDFs) in ANSYS-FLUENT, considering hydrate growth as a porous medium. Simulations were validated by experimental estimations, where the measurements were conducted by using a cylindrical cell, with radially positioned thermocouples to acquire temperatures throughout the experimental setup. The objective was to investigate hydrate growth from the wall in a water-dominated system using a tetrahydrofuran hydrate solution. Three bath temperatures (-1.0ºC, -3.0ºC, and 1.0ºC) and a stoichiometric tetrahydrofuran hydrate concentration of 1:17 were utilized. From the thermal study, the temperature data was analyzed verifying the value of the energy barrier resistance parameter of 6E-06. Additionally, two cases from the literature for two different geometries (cylindrical and rectangular domains) were considered for further numerical verification. The experimental cases show that the formation of hydrate acted as a thermal insulator, avoiding efficient heat removal from the hydrate layer. Consequently, the growth of the hydrate layer was delayed, aligning with the predictions of the numerical model. The integrated approach of the presented model offers a realistic representation of tetrahydrofuran hydrate growth, shedding light on the underlying phenomena involved.*

Keywords: *energy-barrier-resistance crystal growth, THF-hydrate, numerical-simulations.*

1. INTRODUCTION

Over the years, the offshore industry has been striving to meet the increasing demands for oil and gas. In response to this, the oil and gas sector is expanding its production processes to deep-water regions. These areas are characterized by high-pressure and low-temperature conditions. In such conditions, the production activities involving oil and gas often lead to the formation of hydrates. Hydrates are crystalline solids that resemble ice and are formed when gas and water associated with oil interact. These hydrates can cause blockages in pipelines, resulting in significant financial losses for the industry.

There are three main hydrate structures: I, II, and H, which depend on the nature and size of the gas molecule involved. In oil and gas production, methane, ethane, and propane are prominent hydrate-forming gases. Among these, methane is the most common, accounting for approximately 90% of the gases found in oil and gas production. This one is also the primary hydrate former and the main cause of hydrate blockages in pipelines. Consequently, it has been studied frequently their physical and chemical properties, with a focus on their molecular structure. At the molecular level, methane hydrates have a crystalline structure consisting of 16 small cages and 8 large cages, known as structure sII. In this structure, methane molecules predominantly occupy the large cages (Sloan and Koh 2007).

In addition to methane, other molecules, such as tetrahydrofuran (THF), can also form the sII crystalline structure. Researchers often opt for THF as a hydrate former due to its strong affinity with water under atmospheric conditions, providing a simpler system for study compared to high-pressure systems.

To comprehend gas hydrate formation, empirical-mathematical models aiming to predict the process have been developed. Their formation is considered a crystallization process, wherein the formation of nuclei plays a crucial role in facilitating their continuous growth (Sloan and Koh 2007). The nucleation process is stochastic in nature, prompting several studies to employ simplified analyses that focus on studying the growth process, assuming a successful nuclei formation (Englezos et al. 1987).

Among the studies on the hydrate growth process mathematical models based on the heat transfer (Uchida et al. 1999) the mass transfer (Hanley et al. 1989) and the chemical kinetics (Vysniaukas and Bishnoi 1983) can be found. The models based on heat transfer consider the direct effect of the heat removal from the hydrate growth on their growth rate. It considers the difference between the hydrate melting temperature and bulk cooling temperature as the driving force. This differs from the models based on mass transfer, which use the gradient concentration of the hydrate forming between the regions of hydrate formation and bulk solution to calculate their growth rate. On the other hand, the models based on chemical kinetics evaluate the hydrate forming consumption along the growth process by adjusting a kinetic parameter as a function of experimental data to determine the gas hydrate growth rate. However, the separate study of heat transfer, mass transfer and chemical kinetic models represents a limitation to the understanding of the growth process.
This study focuses on investigating the processes involved in the formation of tetrahydrofuran (THF) hydrates. To achieve this, a numerical model is developed, which incorporates an analytical model proposed. The present proposal is establishing relationships among these factors, providing a comprehensive understanding of the growth process and the relation between heat transfer, mass transfer, and chemical reactions.

2. MATHEMATICAL MODEL

During hydrate growth, heat is released and transported from the hydrate-solution interface to the bulk solution, consequently increasing the energy of the target molecule (Fig. 1a). This energy increase, called potential relief, encompasses various forms of energy, such as translational, vibrational, and rotational energies; initially understood as interface resistance. However, in a second scenario, the long-range attractive forces between the target molecule (higher potential energy) and the vacant cavities within the crystalline network (lower potential energy) induce Brownian motion, guiding the target molecule towards the structured lattice due to the potential gradient (Wu et al. 2014).

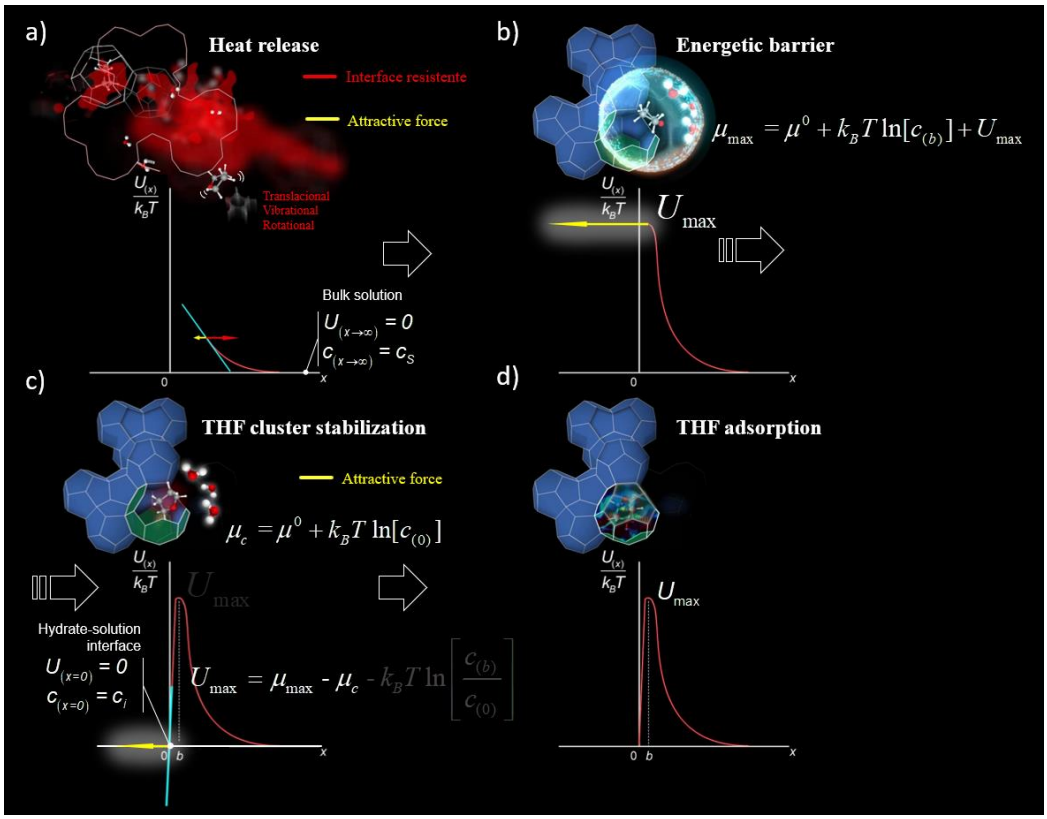

Figure 1. Hydrate formation representation as transition state of molecular substances

So, the hydrate-solution interface advances, the target molecule reaches a state of maximum potential relief U_{max} without any net repulsive force (Fig. 1b). This step represents the energetic barrier of the process. Up to this point, the attractive force has reached its maximum due to the potential gradient between the higher potential of the energized target molecule and the lower potential of the vacant cavity. This results in a reduction of the energy of the target molecule (Fig. 1c). Consequently, the binary clusters can adopt a stable configuration, preparing them for coupling with the crystalline structure. Finally, the adsorption process takes place (Fig. 1d).

To model the THF adsorption rate analytically, the proposed approach begins by defining the chemical potential for the THF species as:

$$\mu(T,x) = \mu^0(T) + k_B T \ln[c_{(x)}] + U_{(x)} \tag{1}$$

where $\mu^0(T)$ is the chemical potential of pure specie, standard state (*J/molecule*); k_B the Boltzmann constant (*J/K-molecule)*; the THF concentration (*molecules/m³*); and the last term $U_{(x)}$ is added in order to model the potential relief (*J/molecule*) above discussed.

Referring to Eq. (1) and evaluating the scenarios depicted in Fig. 1b and Fig. 1c, the following expressions can be deduced:

$$\mu_{\max}(T,b) = \mu^0(T) + k_B T \ln[c_{(b)}] + U_{\max} \tag{2.a}$$

$$\mu_c(T,0) = \mu^0(T) + k_B T \ln[c_{(0)}] \tag{2.b}$$

where each one represents the maximum chemical potential ($\mu_{\max}$) at a distance b and the chemical potential of the stable cluster rearranged at the hydrate-solution interface (μ_c). Then, by subtracting both expressions and considering the analysis of the same molecule in two different locations without mass accumulation at the hydrate solution-interface ($c_{(b)} = c_{(0)}$), the following expression is obtained:

$$U_{\max} = \mu_{\max} - \mu_c \tag{3}$$

where $U_{\max}$ can be interpreted as the energy released by the THF molecule during the stabilization process of the cluster.

In order to associate the the weak long-range attraction force arising from a potential gradient between the position of the target molecule and a reference point (Fig. 1a). The net force per mass unit is estimated based on the chemical potential gradient, which reflects the spontaneous movement of matter. This relationship is mathematically expressed using the generalized Fick law by Eq. (4).

$$J_{THF} = -\frac{c_{(x)} D}{k_B T} \frac{d\mu}{dx} \tag{4}$$

where J_{THF} (*molecules/m²-s*) is the flux of THF molecules with concentration $c_{(x)}$ (*THF molecules/m³-solution*); D is the diffusion coefficient (*m²/s*); T is the temperature (*K*); x is the position coordinate along the crystal growth direction (*m*). Then mathematical manipulations of Eq. (4) result:

$$J_{THF} = -\frac{D}{\Lambda} e^{\left(-\frac{U_{max}}{k_B T}\right)} \left(c_S - c_i\right) \tag{5}$$

Then, taking not mass accumulation into account at hydrate-solution interface the spontaneous adsorption process carries on to finally the hydrate growth. In that sense the adsorption rate it is the same to the flux of THF J_{THF} . Now the THF hydrate growth rate could be obtained by following stoichiometric equation:

$$1\ THF + 17 H_2O \rightarrow 1\ THF\text{-}Hydrate \tag{6}$$

Eq. (6) means that to produce 1 molecule of THF hydrate, 1 molecule of THF and 17 molecules of water are necessary. In other words, it is necessary to absorb 1 molecule of THF to produce 1 molecule of THF hydrate. Therefore, the adsorption rate J_{THF} and the hydrate growth rate R_H could be compared to the relation of 1:1 and can be considered the opposite value of Eq.5. Based on the theory of the kinetic equilibrium (Chernov 2012) we can determine the THF concentration at hydrate-solution interface c_i in function of thermodynamics parameter as the changes in the free energy ($\Delta\bar{G}$), enthalpy ($\Delta\overline{H}$), and entropy ($\Delta\bar{S}$). Also, the free energy change can be expressed by an approximation of the

free energy change during the crystallization process (Thompson and Saepen 1979). So, from Eq. (5) the hydrate growth rate can be rewritten as:

$$R_H = f\frac{D}{\Lambda}\left[c_S - qe^{\left(\frac{\Delta\bar{H}\left(T_{ref}-T\right)}{k_B T T_{ref}}\right)}\right] \Rightarrow f = e^{\left(-\frac{U_{max}}{k_B T}\right)} \tag{7}$$

where q (*THF molecules/m³-hydrate*) is the molar concentration of the THF molecules adsorbed at the hydrate-solution interface, and f (-) is the energy barrier resistance for the hydrate growth based on transition state of molecular substances theory (Chernov 2012).

The analytical model in Eq. (7) presents a similarity with the model proposed by Kirkpatrick 1975 for determinate the crystal growth rate from melts and recently by Mazhukin et al. (2017) for the kinetic melting and crystallization of superheated and supercooled metals. For THF hydrates, Yagasaki et al. (2016) used an identical expression too. All those works cited, present a limitation in explain the nature of the parameter f derived mathematically in this work. In this manner, the primary focus of model verification lies on this parameter, which is dependent on the potential relief $U_{\max}$. The energy release by the THF molecule to form a stable cluster at the hydrate-solution interface, as derived in Eq. (3), was determined using values obtained from Molecular Dynamic Simulations conducted by Liu et al. (2019).

3. EXPERIMENTAL SETUP

The experimental methodology used for monitoring the radial growth of hydrates involved a distribution of thermocouples. The cell, schematically shown in Fig. 2, is an acrylic cylinder with 12.6 cm height, 0.5 cm thickness and 14.0 cm diameter. The cell is submerged in a 50 wt. % monoethylene glycol thermal bath that could be set to different sub-cooling levels. It was used THF-water solution (molar ratio of 1:17) and the temperatures into the cell are monitored by five thermocouples (one HSTC-TT-K-24S-72 and four TJ60-CASS-116U-4, OMEGA) which are submerged until half height of the liquid solution, distributed along the radius. The thermocouples are placed equidistant (17.5 mm) from the wall to the center inside the cylinder to determine the temperature distribution of the hydrate film. Additionally, two thermocouples are positioned outside the cylinder, immersed in the thermal bath, to measure the temperatures on the external wall and in the bath. In the present work, the thermocouple, which is detailed in Fig. 2, is used for the numerical model verification.

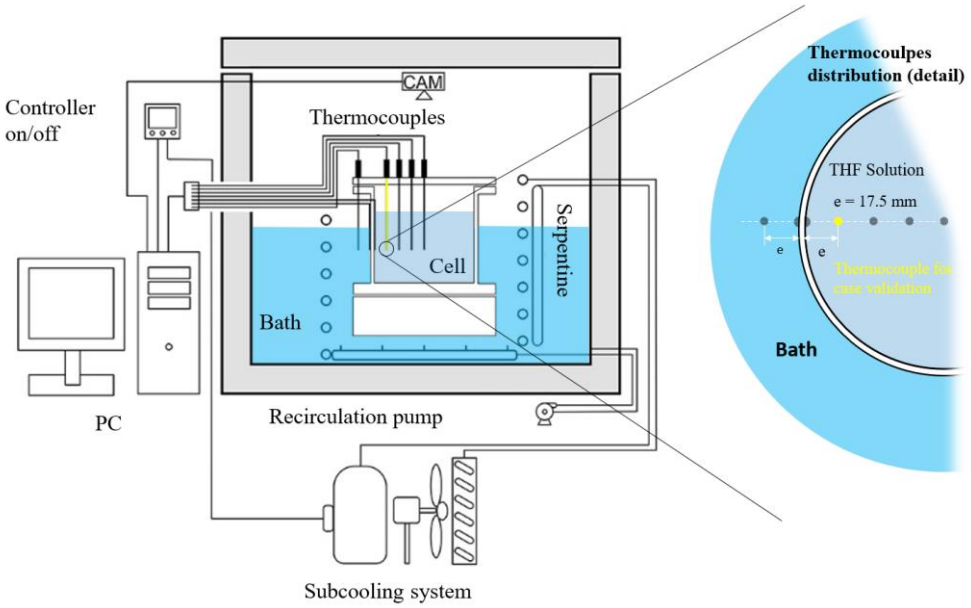

Figure 2. Experimental setup

The experiments involve a solution of THF and deionized water, which was colored with a blue dye. The addition of the dye served the purpose of enhancing the visualization of the porous structure since the dye molecules are larger than

the sII hydrate cavities, thereby maintaining the crystalline nature of the hydrate. Once the solution was poured into the experimental cell. Each experimental run commenced with the setting of the bath temperature and the initiation of temperature recording, with data being acquired every minute.

4. NUMERICAL MODEL

The numerical study in this work employs the energy equation described in Eq. (8).

$$\frac{\partial}{\partial t}\left[\varphi\rho_S E_S + (1-\varphi)\rho_H E_H\right] = \nabla.\left(k_{eff}\nabla T\right) - \Delta\overline{H}\,\dot{R}_H \tag{8.a}$$

$$E_{(S/H)} = \int_{T_{ref}}^{T} c_{P(S/H)}\,dT \tag{8.b}$$

$$k_{eff} = \varphi k_S + (1-\varphi)k_H \tag{8.c}$$

where E is the energy (kJ/kg); φ is the hydrate porosity, c_p is the specific heat capacity; $\Delta\overline{H}$ is the latent heat of formation (J/mol); $\dot{R}_H$ is the hydrate growth rate ($mol/(m^3{\cdot}s)$), k is the thermal conductivity ($W/(K{\cdot}m)$), k_{eff} the effective thermal conductivity ($W/(K{\cdot}m)$) and the subscripts S, H refer to the solution and to the hydrate respectively.

$$\frac{\partial}{\partial t}\left[(1-\varphi)\rho_H\right] = \dot{R}_H M_H \tag{9}$$

where, M_H is the hydrate molar weight (kg/mol) and the source term is given by $\dot{R}_H M_H$ ($kg/(m^3{\cdot}s)$).
The growth of the hydrate is treated as that of a porous medium, where we consider the interstitial area, which is represented by the transverse area perpendicular to the growth direction within the volume control. Consequently, the analytical model is adapted to the numerical model through the use of the form parameter as;

$$\dot{R}_H = \left[\frac{A_{SP}}{V^{cv}}\right] f \frac{D}{\Lambda}\left[c_S - qe^{\left(\frac{\Delta\bar{H}\left(T_{ref}-T\right)}{k_B T T_{ref}}\right)}\right] \tag{10}$$

where $\dot{R}_H$ is the hydrate growth rate per volume unit ($mol\ THF\text{-}hydrate/(m3{\cdot}s)$), A_{SP} is the superficial area of the representative porous media (m^2) and V^{cv} is the volume of the control volume (m^3).

The proposed model was validated using a numerical domain that consisted of an axisymmetric 3D configuration. The boundary conditions corresponding to this domain are illustrated in Fig. 3.

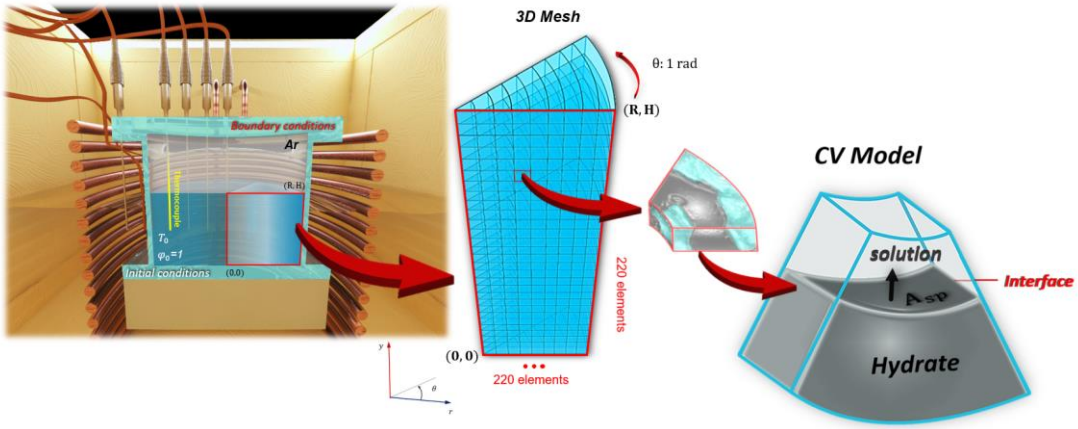

Figure 3. Computational domain (boundary and initial conditions)

The resolution of the system of Eqs. (6)-(9) is defined via the following boundary depicted in Fig.3:

$$y = H \Rightarrow \frac{\partial T}{\partial y} \approx 0 \qquad \frac{\partial \varphi}{\partial y} = 0 \tag{11}$$

$$r = R \Rightarrow T_{r=R} = T_W \qquad \frac{\partial \varphi}{\partial r} = 0 \tag{12}$$

$$y = 0 \Rightarrow T_{y=-e} = T_B \qquad \frac{\partial \varphi}{\partial y} = 0 \tag{13}$$

where a zero heat flux was considered, Eq. (11); for the lateral wall of the cylinder a transient function via UDF using a data registered by the thermocouple T_W was defined, Eq. (12), and for the cylinder base, the bath temperature (thermocouple T_B) was imposed, considering a wall thickness e of 7 cm, Eq. (13).

The initial condition for the THF hydrate growth assumes the unity as the initial system porosity, meaning that all the domain in the solution composition has no presence of hydrate and, for the initial temperature of the system, the experimental observations indicate that the hydrate growth starts with a temperature of approximately 4.1°C. The physical properties used during the simulation are specified in Table 1.

Table 1. THF properties:

	Properties	Unit	THF Hydrate	THF + H2O
R	Internal radius of cell	mm	70.0	
p	Pressure	bar	1.0	
T_{ref}	Reference temperature (equilibrium)	K	277.55[(1)]	
$\Delta T_{min\text{-}wall}$	Wall minimum sub cooling	K	0.4[(2)]	
$\Delta T_{min\text{-}bulk}$	Bulk minimum sub cooling	K	0.0[(2)]	
ρ	Density	kg/m³	970.76[(3)]	970.76[(3)]
c_p	Specific heat capacity	J $kg^{-1}K^{-1}$	2123[(4)]	4210[(1)]
M	Molar weight	kg/mol	0.3783 [(5)]	0.0210[(5)]
$\Delta\bar{H}$	Latent heat formation	kJ/mol	-100[(4)]	-
k	Thermal conductivity	W $m^{-1}.K^{-1}$	0.525[(6)]	0.562[(6)]
φ_F	Final hydrate porosity	-	~0.1	-
Λ	THF free path	m	-	6.5E-10[(7)]
c_s	THF Concentration at bulk solution	THF molecules⁄m³ solution	-	2565.67[(3)]
ϥ	THF concentration at hydrate	THF molecules⁄m³ hydrate	2565.67[(3)]	-

[(1)] Iida et al. (2000), [(2)] This work (experimental), [(3)] Calculated, [(4)] Leaist et al. (1982), [(5)] Calculated, [(6)] Ross e Andersson (1982). [(7)] Wu et al. 2014.

5. MODEL VERIFICATION

A uniform mesh with 220x220 elements and a time step of 10 seconds was used for the numerical validation. The model validation aimed to analyze the energy barrier resistance (f) under three scenarios: 1.0ºC, -1.0ºC and -3.0ºC. Through an optimization routine, the variable under verification was estimated to be 6 E-06 (-), indicating an energy release of 4.6068E-20 per molecule, as described in Eq. (7).

In Fig. 4, the temperature drop on thermocouple can be observed for both experimental and numerical results after maintaining a uniform temperature of 4.1ºC. In these scenarios, the hydrate reaches each thermocouple due to radial growth from the lateral cylinder wall. As a result, the numerical results exhibit a strong agreement with the experimental.

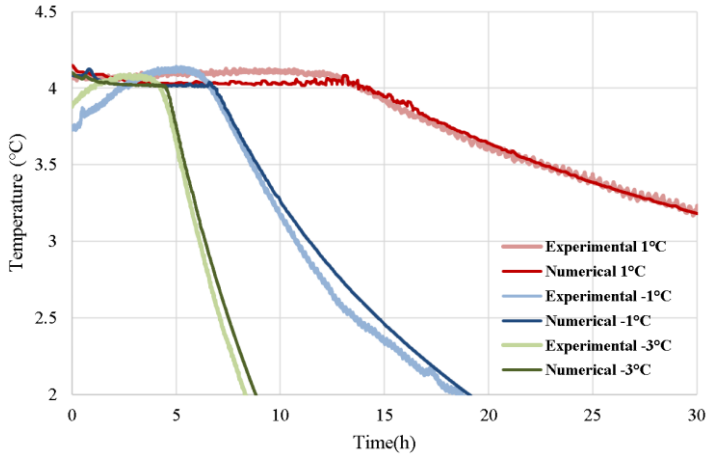

Figure 4. Thermal study, thermocouple verification.

Tables 2 display the temperature drop in thermocouple over time, along with their respective absolute errors in model validation. The absolute deviation error (AD) between the experiments and the numerical model was calculated using the following equation:

$$AD = \frac{|\Phi_E - \Phi_N|}{\Phi_E}.100\% \tag{15}$$

where Φ_E and Φ_N are the experimental and numerical data respectively.

Table 2. The absolute deviation errors.

Bath temperature (°C)	Experimental time (h)	Numerical time (h)	AD Error (%)
1.0	13.00	13.24	1.85%
-1.0	6.82	7.00	2.64%
-3.0	4.21	4.57	8.55%

Table 2 reported a maximum absolute deviation (AD) error of 8.55% for the case with bath temperatures of -3.0ºC. This discrepancy could be attributed to the heat released during hydrate growth from the cylinder base, which is transported to the bulk solution, increasing its temperature and subsequently retarding the radial growth process. Additionally, it was observed that growth times were shorter for the high cooling system (bath temperatures of -3.0ºC) compared to the low cooling system (bath temperatures of 1.0ºC).

Up to the energy barrier resistance (f), a physical interpretation can be derived from the values obtained in the Molecular Dynamic Simulations conducted by Liu et al. (2019).

Table 3. Energy barrier resistance estimation from Liu et al. (2019), number of water molecules at hydrate- solution interface.

Nº water molecules	***E_{sta}* (J/molecule)**	***f (E-06)***
1	2.83586E-20	610.84952887
2	3.46071E-20	119.58062719
3	4.24578E-20	15.40915566
4	**4.61428E-20**	**5.88950962**
5	5.15902E-20	1.42105211
6	5.57559E-20	0.47910172
7	6.04022E-20	0.14248294
8	6.52087E-20	0.04063845
9	6.77722E-20	0.02081438
10	7.17777E-20	0.00731715

From Table 3, it can be observed that the energy barrier resistance, which is approximately the value obtained through the optimization procedure, represents the stabilization of the THF molecule with four water molecules at the hydrate-solution interface. The parameter exhibits the same order of magnitude (E-06) typical for crystal growth from concentrated solutions, showing its consistency.

Furthermore, to conduct additional numerical verification, two cases were considered to examine the independence of the energy barrier resistance from the experimental setup. Figure 5 displays the numerical results based on previous experimental studies from the literature, considering THF solutions with a 1:17 molar concentration for two distinct systems. Detailed descriptions of the boundary conditions and the specific cases studied in each work are provided.

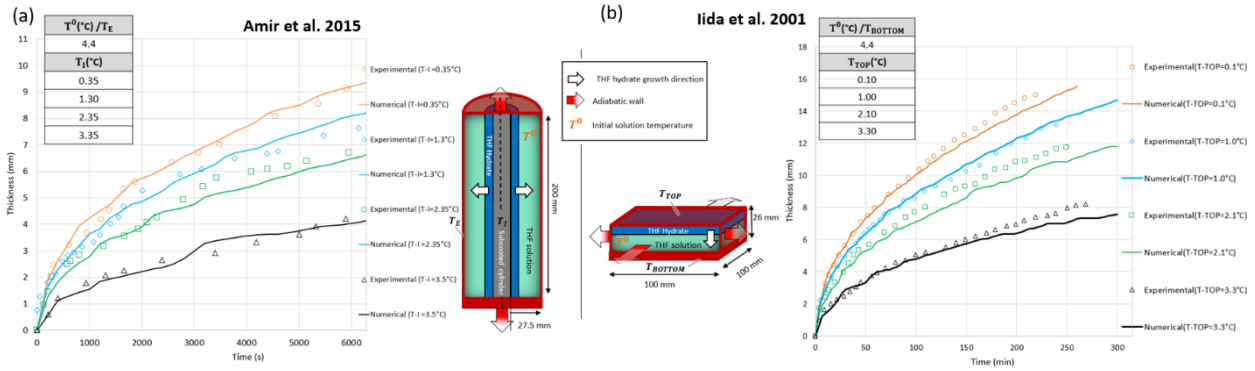

Figure 5. Model verification

Fig. 5(a) show the numerical verification based on the study conducted by Amir et al. (2015). In the second scenario, the investigation explores another instance of hydrate growth on a planar subcooled wall, utilizing the experimental model proposed by Iida et al. (2001). Tables 4 and 5 present the maximum and minimum errors obtained from the numerical results for both cases.

Table 4. Numerical errors (Amir et al. 2015).

T_I (°C)	Min error (%)	Max error (%)
0.35	0.093	15.444
1.3	2.625	7.148
2.35	0.148	10.5
3.5	0.474	15.446

Table 5. Numerical errors (Iida et al. 2001).

T_{TOP} (°C)	Min error (%)	Max error (%)
0.10	0.155	3.722
1.00	0.017	3.922
2.10	1.982	7.692
3.30	3.604	10.840

6. CONCLUSIONS

The numerical model established a correlation between the local mass transfer, elucidated by Brownian motion of THF molecules at the hydrate-solution interface, kinetic adsorption process, and heat transfer. As a result, the final expression for the hydrate growth rate bears resemblance to models constrained by heat transfer, commonly used to estimate the hydrate growth rate.

Numerical model developed shows consistency with other scenarios of THF hydrate growth, as observed in previous studies by Amir et al. (2015) and Iida et al. (2001). The verified energy barrier resistance model of 6 E-06 (-) aligns with typical values observed for crystal growth from concentrated solutions. The interpretation of the physical meaning of this parameter was derived from Molecular Dynamic Simulations, which revealed that the THF molecule becomes trapped

and needs to overcome the energy barrier resistance in order to form a stable cluster at the hydrate-solution interface with four water molecules.

Moreover, in all cases, the influence of heat transfer on the growth process was determinant. The presence of THF hydrate as an insulating barrier substantially hindered heat removal from the bulk solution, resulting in a reduction in hydrate growth. The cooling system employed also played a crucial role in hydrate growth, as shorter growth times were observed for high cooling systems compared to low cooling systems.

7. REFERENCES

Amir, et al. "Experimental and computational study on clathrate hydrate of tetrahydrofuran formation on a subcooled cylinder." International Journal of Refrigeration 59 (2015): 84-90.

Chernov, Aleksandr Aleksandrovich. Modern crystallography III: crystal growth. Vol. 36. Springer Science & Business Media, 2012.

Englezos, P., et al. "Kinetics of formation of methane and ethane gas hydrates." Chemical engineering science 42.11 (1987): 2647-2658.

Hanley, H. J. M., et al. "The melting curve of tetrahydrofuran hydrate in D_2O." International Journal of Thermophysics 10 (1989): 903-909.

Kirkpatrick, R. James. "Crystal growth from the melt: a review." American Mineralogist: Journal of Earth and Planetary Materials 60.9-10 (1975): 798-814.

Liu, Jinxiang, et al. "Tetrahydrofuran (THF)-Mediated Structure of THF·(H2O) n= 1–10: A Computational Study on the Formation of the THF Hydrate." Crystals 9.2 (2019): 73.

Mazhukin, V. I., et al. "Kinetic melting and crystallization stages of strongly superheated and supercooled metals." Mathematical Models and Computer Simulations 9 (2017): 448-456.

Sloan Jr, E. Dendy, and Carolyn A. Koh. Clathrate hydrates of natural gases. CRC press, 2007.

Thompson, Carl V., and Frans Spaepen. "On the approximation of the free energy change on crystallization." Acta Metallurgica 27.12 (1979): 1855-1859.

Tomoyuki, I. A. "Formation and dissociation of clathrate in stoichiometric tetrahydrofuran-water mixture subjected to one-dimensional cooling or heating." Chemical Engineering Science 56.4 (2001): 747-4.

Uchida, Tsutomu, et al. "Microscopic observations of formation processes of clathrate-hydrate films at an interface between water and carbon dioxide." Journal of crystal growth 204.3 (1999): 348-356.

Vysniauskas, Anthony, and P. R. Bishnoi. "A kinetic study of methane hydrate formation." Chemical Engineering Science 38.7 (1983): 1061-1072.

Wu, Jyun-Yi, et al. "Molecular dynamics study on the equilibrium and kinetic properties of tetrahydrofuran clathrate hydrates." The Journal of Physical Chemistry C 119.3 (2015): 1400-1409.

Yagasaki, Takuma, Masakazu Matsumoto, and Hideki Tanaka. "Mechanism of slow crystal growth of tetrahydrofuran clathrate hydrate." The Journal of Physical Chemistry C 120.6 (2016): 3305-3313.

8. RESPONSIBILITY NOTICE

The author(s) is (are) the only responsible for the printed material included in this paper.